Ore Geology Reviews 131 (2021) 104043

Contents lists available at ScienceDirect

Ore Geology Reviews

journal homepage: www.elsevier.com/locate/oregeorev

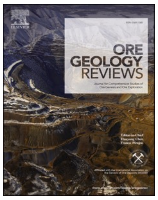

Thermodynamic properties of ruthenium (IV) chloride complex and the transport of ruthenium in magmatic-hydrothermal fluids

Haibo Yan [a,b,c,f], Weidong Sun [d,e,f], Junfeng Liu [g], Xianglin Tu [a,b], Xing Ding [a,b,f,*]

[a] State Key Laboratory of Isotope Geochemistry, Guangzhou Institute of Geochemistry, Chinese Academy of Sciences, Guangzhou, 510640, China
[b] CAS Center for Excellence in Deep Earth Science, Guangzhou, 510640, China
[c] CAS Key Laboratory of Mineralogy and Metallogeny, Guangzhou Institute of Geochemistry, Chinese Academy of Sciences, Guangzhou, 510640, China
[d] Center for Ocean Mega-Science, Chinese Academy of Sciences, Qingdao, 266071, China
[e] Center of Deep Sea Research, Institute of Oceanography, Chinese Academy of Sciences, Qingdao, 266071, China
[f] University of the Chinese Academy of Sciences, Beijing, 100049, China
[g] School of Earth Science and Resources, Chang'an University, Xi'an, 710054, China

ARTICLE INFO

Keywords:
Ru-Cl complex
Hydrolysis
Transport
Hydrothermal fluids
Submarine hydrothermal fluids

ABSTRACT

Thermodynamic properties of platinum-group element (PGE) coordination complexes are significant for our understanding of PGE mobilization, transport, and deposition in hydrothermal fluids. This study conducted hydrolysis experiments of ruthenium (IV) chloride complex (K_2RuCl_6) at temperatures of 200–600 °C and water pressure of 100 MPa, combined with related geochemical modeling, to quantitatively investigate the thermodynamic behavior of the Ru-Cl complex in magmatic-hydrothermal fluids. The results show that the hydrolysis reactions of $[RuCl_6]^{2-}$ get equilibrium within 24 hours at 200 °C and have positive temperature dependence. The cumulative hydrolysis constants (K) calculated for the reactions fit well on a linear correlation with temperatures (T, Kelvin):

$\ln K = (42.95 \pm 4.13) - (56205 \pm 2594)/T$.

Based on the cumulative hydrolysis constants obtained, we established a preliminary model to decipher the quantitative relationship among the temperature, pH, total chlorine concentration, and the mobility of the Ru-Cl complex in natural Cl-bearing hydrothermal fluids. The calculation results demonstrate that Ru could be mobile in the Cl-bearing (0.05–0.5 wt%), low to moderate temperature ($\leq$550 °C), and acidic ($pH \leq 4$) fluids, and be highly mobile in the Cl-rich (0.5–20 wt%), acidic - weakly alkaline fluids. The fluid's pH and total chlorine concentration dominate the Ru-Cl complex's stability and the Ru transport. Therefore, dilution of ambient seawater on the hydrothermal fluids and plumes related to the magmatic-hydrothermal vent systems is the geochemical barrier, which is advantageous to PGE precipitation and mineralization. Furthermore, this study highlights the importance of metal source for the PGE mobilization and deposition and suggests that the source's deficiency substantially limits the PGE mobilization, transport, and deposition, resulting in the scarcity of hydrothermal PGE deposits in the crust.

1. Introduction

Platinum-group elements (PGEs: Pt, Pd, Os, Ir, Ru, Rh), a kind of rare and precious metal resource, are chalcophile and siderophile, thus are preferentially incorporated into sulfide and reserved in the Earth's core and mantle, resulting in the deficient concentrations in the Earth's crust ($\leq$50 ppt) (Li, 1976; Mcdonough and Sun, 1995; Gao et al., 1998; Yan et al., 2020a). Due to the geochemical inertness during magma differentiation, PGEs have widely been used as petrogenetic tracers in studying mafic–ultramafic magmatic rocks and ore deposits since the late 1970s (Keays and Davison, 1976; Crocket, 1979; Naldrett, 2004). For example, the PGEs data have been used to constrain the timing of sulfide segregation from magmas (Hoatson and Keays, 1989; Keays, 1995) and internal differentiation of magmatic sulfide liquid pools (Barnes et al., 1997; Naldrett et al., 1997; Barnes and Liu, 2012; Yan et al., 2020a). By contrast, increasing field observations have shown that

---

* Corresponding author at: State Key Laboratory of Isotope Geochemistry, Guangzhou Institute of Geochemistry, Chinese Academy of Sciences, Guangzhou, 510640, China.

E-mail address: xding@gig.ac.cn (X. Ding).

https://doi.org/10.1016/j.oregeorev.2021.104043
Received 28 July 2020; Received in revised form 9 December 2020; Accepted 29 January 2021

PGEs could be enriched through hydrothermal processes in some geological systems, such as the porphyry Cu-Au systems (Auge et al., 2005; Lefort et al., 2011), Cu-Zn massive sulfide deposits (Pašava et al., 2004; Vikentyev et al., 2004, 2014), sediment-hosted base metal deposits (Coveney and Nansheng, 1991; Pasava et al., 2010), and submarine hydrothermal deposits in the mid-ocean ridge regions (Harrar and Stephens, 1984; Mckibben et al., 1990; Huang et al., 2011). These suggest that PGEs are potentially mobile in the hydrothermal fluids.

A few experiments have been conducted to investigate the hydrothermal solubility and mobility of PGEs in fluids (Orlova et al., 1987; Mountain and Wood, 1988a, 1988b; Wood et al., 1989; Gammons and Bloom, 1990; Hsu et al., 1991; Gammons, 1995; Levitin and Schmuckler, 2003; Hanley et al., 2005; Yan et al., 2020a). Compared to lower solubility (several hundred ppb) in HS^--rich fluids, the solubility of PGEs (Pt, Pd, and Os) can be up to several hundred ppm in the Cl-rich fluids at low to moderate temperatures ($\leq$600 °C) and low pressures ($\leq$150 MPa), suggesting that Cl-rich fluids rather than HS^--rich fluids are more favorable to the PGEs dissolution and transport (Orlova et al., 1987; Gammons et al., 1992; Gammons and Bloom, 1993; Pan and Wood, 1994; Xiong and Wood, 2000). Hsu et al. (1991) determined experimentally that the Pd solubility increased gradually with the temperatures rising from 300 to 700 °C in the NaCl-rich fluids with pH = 6 and $f(O_2)$ = NNO, which displays the temperature dependence on the PGE dissolution. It has also been demonstrated that high chloride concentrations in fluids could increase the solubility of PGEs (Pt, Pd, and Rh) obviously, thus promoting the formation of high coordination complex ions, i.e., $PtCl_4^{2-}$, $PtCl_6^{2-}$, $PdCl_4^{2-}$, and $PdCl_6^{2-}$ (Halbach et al., 1989; Wilde et al., 1989; Wood et al., 1992; Gammons, 1995; Xiong and Wood, 2000; Spieker et al., 2002; Levitin and Schmuckler, 2003; Li and Yan, 2013; Brugger et al., 2016). In these cases, high oxygen fugacity could facilitate the formation and stability of higher coordination PGE-Cl complex ions (Gammons, 1995); however, increasing pH could reduce the coordination numbers of PGE-Cl complex ions and decrease the stability of PGE-Cl complexes (Wood et al., 1992; Yan et al., 2020a). Therefore, previous studies believed that PGEs were soluble in Cl-rich fluids. However, their hydrothermal solubility and mobility were restricted by some factors, such as temperature, chloride concentration, oxygen fugacity, and pH (Yan et al., 2020a).

Ruthenium (Ru), one of the PGEs, is usually depleted in the Earth's crust (as low as one ppt) (Yan et al., 2020a). However, in some hydrothermal process involved geological environments, high Ru concentration has been generally observed, such as massive sulfides (up to 6 ppb) from the Uzelginsk deposit in the southern Urals, Russia (Vikentyev et al., 2004), the Cu-rich stockwork ores of the Aguas Teñidas Este (up to 21 ppb) and the Neves Corvo (up to 13 ppb) deposits (Pašava et al., 2007), and the altered sulfides in the Cu/Ni-PGE deposit (1.74–12.14 ppm) (Holwell et al., 2017). In the submarine cold seep and hydrothermal vent systems, ruthenium enrichment can also be observed (Harrar and Stephens, 1984; Mckibben et al., 1990; Huang et al., 2011; Ren et al., 2016). Huang et al. (2011) reported high concentration Ru (up to 0.044 ppb) detected in the hydrothermal fluids of the southwest Indian ridge, which implies Ru transport from the deep mafic magmas to the ocean floor. Moreover, the submarine encrustations generally contain a considerable amount of PGEs, e.g., the polymetallic nodules (up to 14.3 ppb) in the CC zone as well as the Co-rich crust (up to 24.8 ppb) in West Pacific (He et al., 2006; Ren et al., 2016), also displaying Ru transport and deposition in the ocean water. Notably, Chen (1994) and Sassani and Shock (1998) believed that Ru could dissolve into the Cl-bearing fluids to form a series of high coordination Ru-Cl complexes, such as $RuCl_4^{2-}$, $RuCl_5^-$, and $RuCl_6^{2-}$. The formation of these high coordination Ru-Cl complexes is beneficial to the Ru transport and cycle in the Cl-bearing fluids.

Given that Ru is soluble in the Cl-bearing fluids and its mobility is most likely related to the Ru-Cl complexes, the knowledge of these Ru-Cl complexes' thermodynamic properties is a requisite for an unambiguous understanding of the Ru circulation and deposition in the ocean and deep Earth. However, little has been known about the thermodynamic properties of these Ru-Cl complexes so far, especially at elevated temperatures and pressures (Brugger et al., 2016). A significant reason is that most of the Ru-Cl complexes are unstable in fluids and selectively occur in some extreme conditions, thus they are hard to be studied directly. This hinders us from quantitatively studying their thermodynamic properties (Ding et al., 2018). In this paper, we selected potassium hexachlororuthenium (K_2RuCl_6), the stablest and highest coordination Ru-Cl complex present in oxygenated Cl-rich fluids, as the starting material to investigate the hydrolysis behavior of Ru-Cl complexes at 200–600 °C and 100 MPa. By determining the cumulative equilibrium constants of hydrolysis reactions between the complex and water, as well as modeling the mobility of the complex in the natural Cl-bearing hydrothermal fluids by establishing a preliminary quantitative model, we obtained the systematic enthalpy, entropy, and Gibbs free energy values of the hydrolysis reactions. Also, we quantitatively discussed the effects of ambient temperature, pH, and total chlorine concentration in fluids on the Ru-Cl complex's stability and mobility and the Ru cycle in the magmatic-hydrothermal fluids. Thus this study, on the one hand, enriches the thermodynamic database on the metal complex; on the other hand, it also provides new insights into our understanding of the PGE mobilization, transport, and deposition in the Cl-bearing hydrothermal fluids that might happen not only in the subduction zone but in the submarine cold seep and hydrothermal vent systems.

2. Materials and methods

2.1. Starting materials

Potassium hexachlororuthenium (K_2RuCl_6) (99.95 wt%, AR, Macklin Reagent), the stablest chemical among Ru-Cl complexes at room temperature, was used as the starting material of high-temperature and high-pressure experiments. The K_2RuCl_6 sample used is a brown powder with a density of 2.68 g/cm^3 and can readily dissolve in water, alcohol, and acetone to form a brown solution at room temperature and air pressure. The K_2RuCl_6 crystal consists of a Ru-Cl octahedron and two potassium ions (Fig. 1) (Douglas and Ho, 2006; Holovko et al., 2009; Zheng, 2009; Persson, 2016). The Ru-Cl octahedron is composed of a ruthenium atom at the center and six chlorine atoms at the edges. Each atom is bonded to the other by covalent bonds in the Ru-Cl octahedron, while two potassium atoms exist in the lattice of K_2RuCl_6, but are free outside the Ru-Cl octahedrons. Linked by weak ionic bonds, the potassium atoms and Ru-Cl octahedrons can be easily separated to form K^+ and $[RuCl_6]^{2-}$ anion groups in a solution.

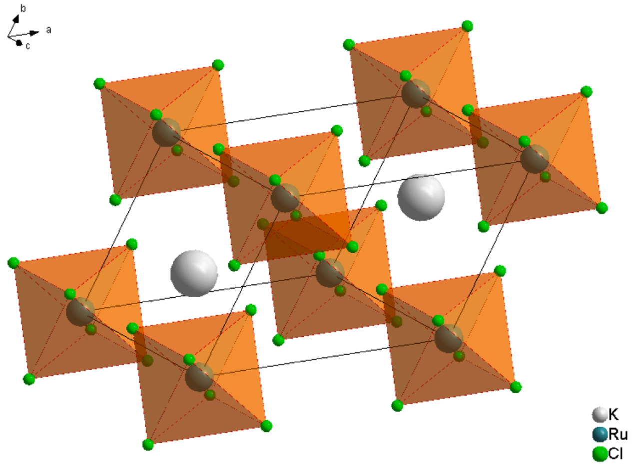

Fig. 1. The crystal structure of potassium hexachlororuthenium (K_2RuCl_6) (Westland, 1963; Douglas and Ho, 2006; Zheng, 2009; Persson, 2016).

2.2. Experimental method and apparatus

The pyrohydrolysis method was used in this study to probe into the stability of the Ru-Cl complex in the hydrothermal fluids. Hydrolysis is a common chemical process that high-valence metal cations, cluster ions, and metal complexes react with water molecules and leading to the dissociation of water molecules and the instability of the metal cations (Holovko et al., 2005, 2009). Therefore, the hydrolysis process plays a destructive role in the dissolution and transport of high-valence metal elements in hydrothermal fluids (Baes and Mesmer, 1981). By this method, the dilute solution containing the Ru-Cl complex was welded into a gold capsule, which was then heated and pressurized to a certain extreme condition. Consequently, a portion of K_2RuCl_6 was hydrolyzed, causing a portion of Ru to precipitate from the solution and a surplus of Cl in the solution. The excess of Cl in the solution generally facilitates the formation of the highest coordination PGE-Cl complex (Levitin and Schmuckler, 2003; Wood et al., 1992; Yan et al., 2020a). It, therefore, ensures that the high coordination anion $RuCl_6^{2-}$ is the dominant species in the solution (Chen, 1994; Sassani and Shock, 1998).

First of all, 7.8 mg, 31.4 mg, and 78.4 mg K_2RuCl_6 powder were weighed using an analytical balance (±0.1 mg, Sartorius, BS124S) and dissolved respectively into 100 mL of deionized water to make 0.0002 $mol·L^{-1}$, 0.0008 $mol·L^{-1}$, and 0.002 $mol·L^{-1}$ aqueous dilute solutions. Then gold capsules with 4 mm diameter and 20–25 mm length were prepared as the reactant container by cleaning with hydrochloric acid (heating to 75 °C for 2 hours), alcohol, and deionized water, following by annealing for 2 hours in a muffle furnace (±1°C, Kejing, KSL-1750X) at 850 °C to ensure no impurities and cracks included. Finally, the prepared reactant containers were filled with different initial Ru solutions of approximately 100uL by the pipette and sealed at both two ends with a tungsten inert gas welding system (PUK U3, Germany), and checked for leaks in an oven (±1°C, Jiangdong, DGG-9070B) at 110 °C for at least 2 hours. The gold capsules without mass differences were used as the samples for subsequent experiments. Usually, at the same conditions, two or three repeated experiments were conducted to verify the repeatability of the experiment result in this study.

All the pyrohydrolysis experiments were conducted by the Tuttle-type cold-seal pressure vessels with 27 mm outer diameter, 6 mm inner diameter, and 250 mm length, using water as the pressure medium, in the hydrothermal laboratory at the Guangzhou Institute of Geochemistry (He et al., 2015a,b). A NiCr-Ni (K-type) thermocouple was used to monitor the temperature with an electronic temperature controller (±5°C) while the pressure was transmitted by water and monitored by gauges (±5 MPa). The oxygen fugacity close to the nickel - nickel oxide (NNO) redox buffer was produced by a nickel filler rod of ~10 cm length, which was placed above the gold capsule when the welded gold capsule was loaded into the bottom of the pressure vessel. After the experiments were finished, a rapid cooling method using an ice-water mixture makes the temperature of the vessels drop to below 100 °C within several seconds and avoids the apparent re-dissolution of precipitates (He et al., 2015a,b). All recycled gold capsules were washed and weighed again to make sure the tightness during the experiments.

2.3. Analytical methods

After the experiments, the products recovered from the gold capsules were processed carefully and analyzed. The reactive solutions were extracted from the gold capsules by a micropipette immediately into a cleaned centrifugal tube and centrifuged at 4500 r/min for 15 minutes to ensure that the precipitates were separated from the solutions. The separated solutions were extracted by micropipettes into 15 mL plastic containers and diluted with a 5% hydrochloric acid solution. Finally, Ru concentrations of the initial solutions and the corresponding recovered reactive solutions were analyzed using a Thermo Scientific iCAP Qc ICP-MS at the State Key Laboratory of Isotope Geochemistry, Guangzhou Institute of Geochemistry, Chinese Academy of Sciences (Guangzhou, China). The standard solution with 10 ppb of Ru determined at the State Key Laboratory of Isotope Geochemistry, Guangzhou Institute of Geochemistry, Chinese Academy of Sciences (Guangzhou, China), was used as the external standard solution for the correction and calibration of the mass spectrometer. Cesium (Cs) was used as the internal standard and was added into the standard and sample solutions to correct instrument fractionation. The detection limit of ruthenium was less than 0.1 ppt, and the precision (two standard deviations) of the analyses was better than 3%.

Following by the extraction of solutions, the gold capsules were cut open and cleaned repeatedly by alcohol and deionized water to ensure the purity of precipitates that adhere to the inner wall of the gold capsule tightly. Then the precipitates were dried in the oven (DGG-9070B) at 60 °C and *in-situ* analyzed by a WITec alpha 300R Confocal Laser Raman Spectrometer with a Zeiss microscope (Germany) as well as 488 nm, 532 nm, 633 nm laser generators in the hydrothermal laboratory at the Guangzhou Institute of Geochemistry. During the analysis, the laser power is 10 mW, and the integration time is 5 s, while the laser wavelength is 532 nm.

3. Results and discussions

3.1. Reaction equilibration of the hydrolysis experiments

To investigate the equilibration time of the hydrolysis reaction, we conducted a series of time-series experiments running for 1 hours to 48 hours at 200 °C and 100 MPa with an initial K_2RuCl_6 concentration of 0.002 mol/L. The analysis of solid precipitates shows that only the RuO_2 solid was formed during the experiments (Fig. 2), suggesting no tetravalent Ru was reduced into trivalent or bivalent ones at the experimental conditions. The cumulative hydrolysis reaction can be thus addressed as:

$$RuCl_6^{2-} + 2H_2O \rightarrow RuO_2\downarrow + 2Cl^- + 4HCl. \quad (1)$$

This reaction can be considered as a progressive nucleophilic substitution of an anion Cl^- by the hydroxyl OH^- derived from the water molecules' dissociation (Ding et al., 2018).

Time-series experimental results show that the concentrations of residual Ru decrease continuously within 24 hours and remain steady after 24 hours, suggesting the hydrolysis reaction reaches equilibrium within 24 hours at 200 °C and 100 MPa (Table 1 and Fig. 3). Considering that elevated temperatures could usually accelerate the hydrolysis reaction (Mo, 2004), the exact equilibration time of the hydrolysis

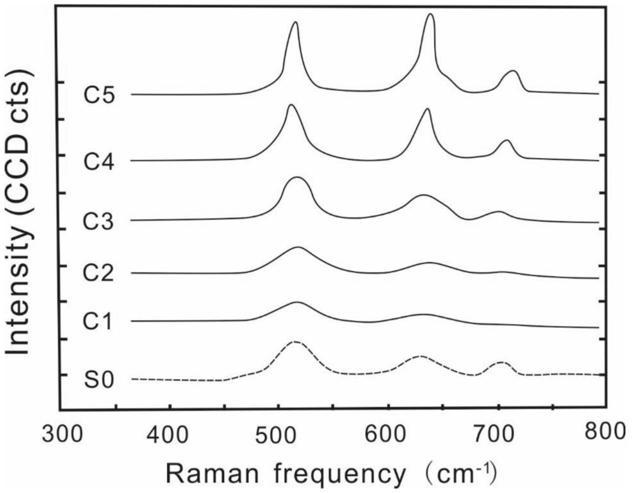

Fig. 2. Raman spectra of the experimental precipitates with initial Ru concentration of 24.4 ppm at different temperatures: (C1) $T = 200$ °C, (C2) $T = 300$ °C, (C3) $T = 400$ °C, (C4) $T = 500$ °C, (C5) $T = 600$ °C. The standard Raman spectum of RuO_2 (S0) is from (Mar et al. (1995)) .

Table 1
Results of K_2RuCl_6 hydrolysis at different temperatures and initial Ru concentrations, and the corresponding cumulative hydrolysis constants.

Run No.	Temperature (°C)	Pressure MPa	Time (hours)	Initial Ru concentrations ppm	Residual Ru concentrations ppm	I mol·L^{-1}	γ(Cl^-) mol·L^{-1}	γ(H^+) mol·L^{-1}	γ($RuCl_6^{2-}$) mol·L^{-1}	Cumulative hydrolysis constant (ln K)
18Ru1-1[a]	200	100	1	192	170					
18Ru1-2	200	100	3	192	72.6					
18Ru1-3	200	100	6	192	11.3					
18Ru1-4	200	100	9	192	1.49					
18Ru1-5	200	100	12	192	0.325					
18Ru1-6	200	100	24	192	0.026					
18Ru1-7	200	100	36	192	0.019					
18Ru1-8	200	100	48	192	0.021					
19Ru1-1	200	100	24	75.7	0.081	0.00449	0.902	0.913	0.670	−69.68
19Ru1-1-1	200	100	24	75.7	2.03	0.00443	0.903	0.914	0.672	−73.15
19Ru1-6	200	100	24	75.7	0.040	0.00449	0.902	0.913	0.670	−68.96
19Ru1-6-1	200	100	24	75.7	0.965	0.00446	0.902	0.914	0.671	−72.27
19Ru1-2	300	100	24	75.7	0.060	0.00449	0.874	0.889	0.594	−50.85
19Ru1-2-1	300	100	24	75.7	0.102	0.00449	0.874	0.889	0.594	−51.39
19Ru1-7	300	100	24	75.7	0.016	0.00449	0.874	0.889	0.594	−49.53
19Ru1-7-1	300	100	24	75.7	1.74	0.00444	0.875	0.889	0.596	−54.45
19Ru1-3	400	100	24	75.7	0.027	0.00436	0.829	0.850	0.486	–32.39
19Ru1-3-1	400	100	24	75.7	0.185	0.00435	0.830	0.850	0.487	−34.33
19Ru1-8	400	100	24	75.7	0.039	0.00436	0.829	0.850	0.486	–32.76
19Ru1-8-1	400	100	24	75.7	2.01	0.00430	0.830	0.850	0.488	−36.95
19Ru1-4	500	100	24	75.7	0.493	0.00202	0.807	0.824	0.435	−25.45
19Ru1-4-1	500	100	24	75.7	0.306	0.00201	0.807	0.824	0.435	−24.96
19Ru1-9	500	100	24	75.7	0.142	0.00201	0.807	0.824	0.435	−24.18
19Ru1-9-1	500	100	24	75.7	0.163	0.00201	0.807	0.824	0.435	−24.32
19Ru1-5	600	100	24	75.7	0.002	0.00150	0.753	0.772	0.332	−20.31
19Ru1-5-1	600	100	24	75.7	0.001	0.00150	0.753	0.772	0.332	−19.69
19Ru1-10	600	100	24	75.7	0.002	0.00150	0.753	0.772	0.332	−20.02
19Ru1-10-1	600	100	24	75.7	0.001	0.00150	0.753	0.772	0.332	−19.08
19Ru2-1	200	100	24	24.4	0.021	0.00145	0.941	0.946	0.789	−79.41
19Ru2-1-1	200	100	24	24.4	0.008	0.00145	0.941	0.946	0.789	−78.45
19Ru2-6	200	100	24	24.4	0.256	0.00144	0.942	0.946	0.789	−82.01
19Ru2-6-1	200	100	24	24.4	0.011	0.00145	0.941	0.946	0.789	−78.79
19Ru2-2	300	100	24	24.4	0.081	0.00144	0.924	0.930	0.734	−62.20
19Ru2-2-1	300	100	24	24.4	2.17	0.00138	0.926	0.931	0.739	−66.38
19Ru2-7	300	100	24	24.4	2.13	0.00138	0.926	0.931	0.739	−66.35
19Ru2-7-1	300	100	24	24.4	0.346	0.00144	0.924	0.930	0.735	−63.76
19Ru2-3	400	100	24	24.4	0.009	0.00143	0.895	0.903	0.649	−41.99
19Ru2-3-1	400	100	24	24.4	0.000	0.00143	0.895	0.903	0.649	−38.59
19Ru2-8	400	100	24	24.4	0.094	0.00143	0.895	0.903	0.649	−44.34
19Ru2-8-1	400	100	24	24.4	0.009	0.00143	0.895	0.903	0.649	−42.00
19Ru2-4	500	100	24	24.4	0.001	0.00081	0.871	0.879	0.581	−26.05
19Ru2-4-1	500	100	24	24.4	0.357	0.00081	0.870	0.879	0.580	–32.02
19Ru2-9	500	100	24	24.4	0.005	0.00081	0.871	0.879	0.581	−27.62
19Ru2-9-1	500	100	24	24.4	0.099	0.00081	0.871	0.879	0.581	−30.67
19Ru2-5	600	100	24	24.4	0.001	0.00048	0.848	0.856	0.524	−25.59
19Ru2-5-1	600	100	24	24.4	0.220	0.00049	0.848	0.856	0.523	−31.03
19Ru2-10	600	100	24	24.4	0.011	0.00048	0.848	0.856	0.524	−28.00
19Ru2-10-1	600	100	24	24.4	0.310	0.00049	0.848	0.856	0.523	−31.39

[a] Runs of 18Ru1-1 ~ 8 are the results of time-series experiments for investigating the equilibration time of the hydrolysis reaction of $RuCl_6^{2-}$.

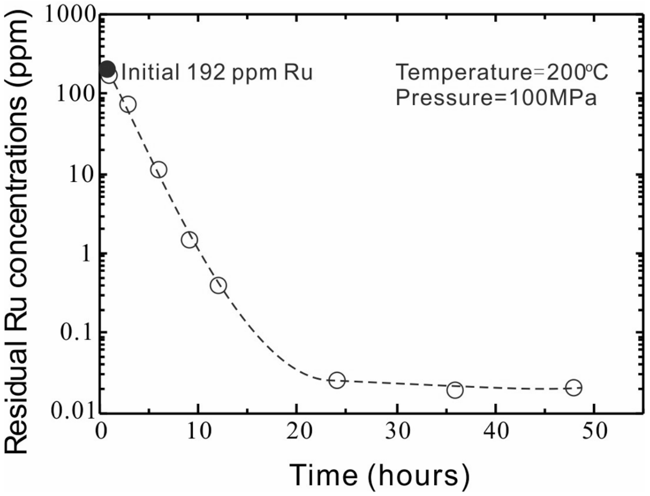

Fig. 3. Residual Ru concentrations of K_2RuCl_6 hydrolysis (200 °C and 100 MPa, initial Ru concentration of 192 ppm) as a function of time. The dotted line represents the decreasing trend of residual Ru concentrations with increasing time. The data suggest that equilibrium was achieved within 24 hours at 200 °C and 100 MPa, with the initial Ru concentration of 192 ppm.

reactions at temperatures of over 200 °C is less than 24 hours. Therefore, all follow-up experiments were conducted with a duration of 24 hours to ensure the hydrolysis equilibrium.

Previous studies on the hydrolysis equilibrium of inorganic complexes have demonstrated that the hydrolysis reaction of the metal complex rather than mineral solubility is more readily to get equilibrium at high-temperature and high-pressure conditions. Similarly, the hydrolysis of Ti-F, Zr-F, and Sn-F complexes reached hydrolysis equilibrium within several to over ten hours at temperatures ranging from 150 to 600 °C and pressures of 50 to 400 MPa (Wang and Chou, 1987; He et al., 2015a; Yan et al., 2020b). By contrast, the equilibration time in the solubility experiments for minerals such as baddeleyite (ZrO_2), molybdite (MoO_3), and tantite (Ta_2O_5) in F-rich fluids was much longer, up to several days or more (Migdisov et al., 2011; Hurtig and Williams-Jones, 2014; Timofeev et al., 2015, 2017). The dissolution rate of minerals is probably controlled by the intricate processes of mineral dissolution, surface energy, and specific surface of minerals; thus, it is much lower at hydrothermal conditions, leading to a longer equilibration time (Ding et al., 2018).

3.2. Temperature dependence of the hydrolysis reaction

Temperature-series experiments have also been conducted at a pressure of 100 MPa and temperatures from 200 to 600 °C using the solutions with various initial Ru concentrations. The residual Ru concentrations in the reactive solutions at temperatures from 200 to 600 °C and the initial Ru concentrations of 24.4 ppm and 75.7 ppm are presented in Table 1. In the experiments with an initial Ru concentration of 75.7 ppm, the residual Ru concentration changes gradually from 2.03 to 0.001 ppm at temperatures increasing from 200 to 600 °C (Fig. 4), suggesting that the temperature largely promotes the hydrolysis of the Ru-Cl complex. This causes most of Ru dissolved in the hydrothermal solutions to precipitate by the reaction Eq. (1). In other experiments with an initial Ru concentration of 24.4 ppm, the residual Ru concentration drops gradually from 0.256 to 0.001 ppm at temperatures increasing from 200 to 600 °C (Fig. 4). The data also suggest that temperature can promote the hydrolysis of $RuCl_6^{2-}$ and negatively affect the stability of Ru-Cl complex in the Cl-rich solutions (Fig. 4).

Strong temperature dependence of hydrolysis reaction is common for inorganic metal complexes (Wang and Chou, 1987; Wang et al., 1993; He et al., 2015a; Yan et al., 2020b). Similar to the Ru-Cl complex, Sn (Ta, Nb, Zr)-F complexes are stable and hardly hydrolyze in solutions at room temperature; however, they hydrolyze greatly with increasing temperatures (Wang and Chou, 1987; Wang et al., 1993; He et al., 2015a; Yan et al., 2020b). Other solubility experiments, as well as thermodynamic calculations, have proposed that the stability of PGE-Cl complexes would decrease with increasing temperatures within a finite temperature range (≤700 °C) (Mountain and Wood, 1988a; Hsu et al., 1991; Wood et al., 1992), consistent with this study. Therefore, the stability and transport of the metal complexes in the hydrothermal fluids could be affected strongly by elevated temperature, which is fundamentally controlled by the hydrolysis behavior of the metal complexes.

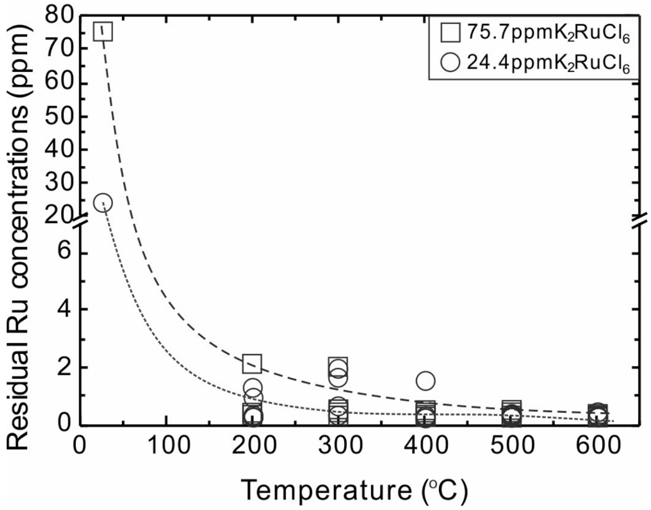

Fig. 4. Experimental results of K_2RuCl_6 hydrolysis at different temperatures and initial Ru concentrations. The dotted lines represent the decreasing trend of residual Ru concentrations with increasing temperature in hydrothermal fluids with various initial Ru concentrations.

3.3. Thermodynamic properties during hydrolysis

Based on the data obtained from the hydrolysis experiments (Table 2), we can calculate those equilibrium constants of the cumulative hydrolysis reaction, as shown in Eq. (1). In this study, the extended Debye-Hückel equation (Helgeson et al., 1981; Tanger and Helgeson, 1988) was used to calculate the activity of ions in the hydrothermal fluids:

$$log_{10}\gamma_i = -\frac{A_\gamma \cdot Z_i^2 \cdot \sqrt{I}}{1 + B_\gamma \cdot \mathring{a} \cdot \sqrt{I}} + b_\gamma \cdot I \tag{2}$$

with A_γ and B_γ being the parameters of the extended Debye-Hückel equation, b_γ the extended parameters, which depends on the nature of the background electrolyte, Z the charge of the ion, and I the true ionic strength when all dissolved components are considered, $\mathring{a}$ the distance of

Table 2
Dissociation constants of $HCl_{(aq)}$ ($logK_{HCl}$), A_γ, B_γ and b_γ at temperatures of 200–600 °C and pressure of 100 MPa. The data are from Mei et al. (2018), Helgeson and Kirkham (1974) and Helgeson et al. (1981).

Temperature	Pressure	$LogK_{(HCl)}$	A_γ	B_γ	b_γ
(°C)	(MPa)	logK	$kg^{1/2} \cdot mol^{-1/2}$	$(kg^{1/2} \cdot mol^{-1/2} \cdot cm^{-1}) \times 10^{-8}$	$(kg \cdot mol^{-1}) \times 10^{-2}$
200	100	2.98	0.7196	0.3592	6.5
300	100	0.95	0.9398	0.378	3.5
400	100	−1.04	1.3262	0.4004	−2.8
500	100	−3.38	2.1872	0.4321	−19.2
600	100	−6.33	3.3281	0.4428	−53.94

closest approach, which is specific to the ion of interest. The values of A_γ and B_γ can be taken from Helgeson et al. (1981) and Helgeson and Kirkham (1974) (Table 2). The value of b_γ was taken from Helgeson et al. (1981) and Migdisov and Williams-Jones (2007), where the best b_γ value for $RuCl_6^{2-}$ was determined in a chemically similar system (Table 2). The distances of closest approach ($\mathring{a}$) were set at 9.0 Å for H^+ (Kielland, 1937; Garrels and Christ, 1965), 3.0 Å for Cl^- (Garrels and Christ, 1965), 3.0 Å for K^+ (Garrels and Christ, 1965), and 4.5 Å for Ru-bearing species such as $RuCl_6^{2-}$ (Kielland, 1937). *I*, the ionic strength of the solution, was calculated from Eq. (3):

$$I = \frac{1}{2}\sum_{i=1}^{n} c_i Z_i^2 \tag{3}$$

where *c* is the molality of species, such as H^+, Cl^-, and $RuCl_6^{2-}$.

The equilibrium constant of Eq. (1) for $RuCl_6^{2-}$ can be expressed as:

$$K = \frac{[HCl]^4 \times [Cl^-]^2}{\left[RuCl_6^{2-}\right]} \tag{4}$$

The dissociation constant of HCl (K_{HCl}) (Mei et al., 2018) and the activity co-efficient (γ) can be introduced into Eq. (4), and it was rewritten as

$$K = \frac{c_{H^+}^4 \gamma_{H^+}^4 \times c_{Cl^-}^6 \gamma_{Cl^-}^6}{c_{RuCl_6^{2-}}\ \gamma_{RuCl_6^{2-}} \times K_{HCl}^4} \tag{5}$$

in which the molarity of $RuCl_6^{2-}$ ($c_{RuCl^{6}_{2-}}$) was determined by the reaction products, and the molarities of H^+ (c_{H^+}) and Cl^- (c_{Cl^-}) were determined by stoichiometric calculation from the equations for the hydrolysis of $RuCl_6^{2-}$ and the ionization of HCl. The calculated results of the ionic strength, activity of ions, and cumulative hydrolysis constants are provided in Table 1.

As shown in Table.1, in the hydrothermal fluids with an initial Ru concentration of 24.4 ppm, the cumulative hydrolysis constant (ln*K*) of $RuCl_6^{2-}$ increases from −82.01 to −25.59 as the temperature increases from 200 to 600 °C. In the hydrothermal fluids with initial Ru concentration of 75.7 ppm, ln*K* increases from −73.15 to −19.08 with increasing temperatures from 200 to 600 °C (Table 1). Therefore, the cumulative hydrolysis constant of $RuCl_6^{2-}$ is significantly controlled by temperature rather than the initial Ru concentration. ln*K* and temperatures show an excellent positive correlation, suggesting that: 1) the hydrolysis reaction between $RuCl_6^{2-}$ and water molecule by Eq. (1) actually happened; 2) no other reactions involving other Ru complexes or tetravalent Ru reduction happened; and 3) the temperatures had critical effects of on the equilibrium constant.

The Van't Hoff Equation was usually used to describe the relationship between the equilibrium constants and temperatures (*T*, Kelvin) in a chemical reaction that actually happens:

$$-lnK = \frac{\Delta_r H_m^{\ominus}}{RT} - \frac{\Delta_r S_m^{\ominus}}{R}. \tag{6}$$

Because the gas constant (R = 8.31451 $J{\cdot}K^{-1}{\cdot}mol^{-1}$) is known, there should be a linear relationship between –ln*K* and 1/*T*. As shown in Fig. 5, a linear relationship between –ln*K* and 1/*T* is presented, and the fitting equation is

$$\ln K = (42.95 \pm 4.13) - -(56205 \pm 2594)/T. \tag{7}$$

$\Delta_r H_m^{\Theta}$ and $\Delta_r S_m^{\Theta}$ of Eq. (1) were inferred to be (467.3 ± 21.56) $kJ{\cdot}mol^{-1}$ and (357.1 ± 34.37) $J{\cdot}mol^{-1}{\cdot}K^{-1}$, respectively. Table 3 shows the calculated and extrapolated cumulative hydrolysis constants (Log *K*) based on Eq. (7) at the temperatures from 50 °C to 800 °C and pressure of 100 MPa.

The change of standard Gibbs free energy ($\Delta_r G_m^{\Theta}$) is a function of the associated $\Delta_r H_m^{\Theta}$, $\Delta_r S_m^{\Theta}$, and temperature (*T*, Kelvin). It is a fundamental equation of state and is used to determine the direction and extent of the reaction in the system:

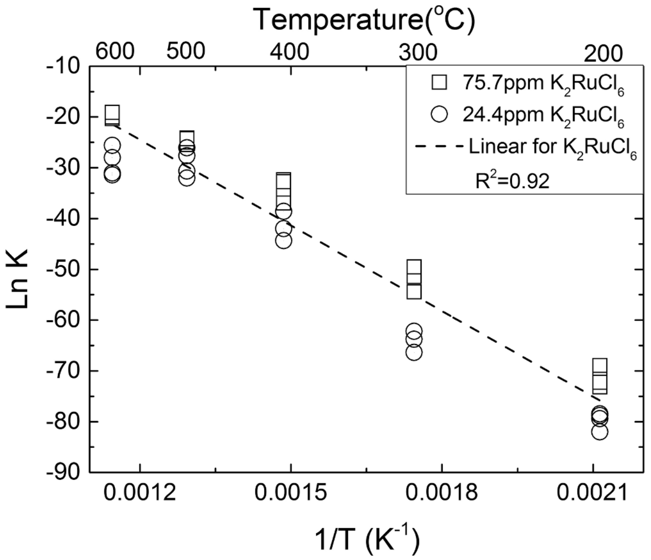

Fig. 5. Temperature-LnK diagram showing the linear correlation between cumulative hydrolysis constants of K_2RuCl_6 and temperature.

Table 3
Calculated cumulative hydrolysis constants (Log *K*), standard formation Gibbs free energy ($\Delta_r G_m^{\Theta}$), and standard deviation of Log *K* and $\Delta_r G_m^{\Theta}$ at temperatures of 50–800 °C and pressure of 100 MPa for the hydrolysis reactions of $RuCl_6^{2-}$.

Temp	Temp	Cumulative hydrolysis constants (Log K)	Standard deviation of Log K	Gibbs free energy ($\Delta_r G_m^{\Theta}$)	Standard deviation of $\Delta_r G_m^{\Theta}$
°C	K			$kJ{\cdot}mol^{-1}$	$kJ{\cdot}mol^{-1}$
50	323.15	−56.88	1.69	351.92	9.47
100	373.15	−46.76	1.23	334.07	10.08
150	423.15	−39.03	0.87	316.21	10.70
200	473.15	–32.94	0.59	298.36	11.31
250	523.15	−28.01	0.36	280.50	11.92
300	573.15	–23.94	0.17	262.65	12.54
350	623.15	−20.52	0.01	244.79	13.15
400	673.15	−17.61	0.12	226.94	13.76
450	723.15	−15.10	0.24	209.08	14.38
500	773.15	−12.92	0.34	191.23	14.99
550	823.15	−11.00	0.43	173.37	15.61
600	873.15	−9.30	0.50	155.52	16.22
650	923.15	−7.79	0.57	137.66	16.83
700	973.15	−6.43	0.64	119.81	17.45
750	1023.15	−5.20	0.69	101.95	18.06
800	1073.15	−4.09	0.74	84.10	18.67

$$\Delta_r G_m^{\theta} = \Delta_r H_m^{\theta} - T\Delta_r S_m^{\theta} \tag{8}$$

Both $\Delta_r H_m^{\Theta}$ and $\Delta_r S_m^{\Theta}$ are quantitative equations of state and can be calculated based on Eq. (6) and Eq. (7). Therefore, $\Delta_r G_m^{\Theta}$ for the Ru-Cl complex's hydrolysis reaction can be calculated and extrapolated to a broader temperature range through the linear relationship between –ln*K* and 1/*T*. As the temperature increases from 50 to 800 °C, $\Delta_r G_m^{\Theta}$ decreases from (351.92 ± 9.47) $kJ{\cdot}mol^{-1}$ to (84.10 ± 18.67) $kJ{\cdot}mol^{-1}$, indicating adverse effects of temperature on $\Delta_r G_m^{\Theta}$ (Table 3).

$\Delta_r G_m^{\Theta}$ of Ru-Cl complex can be controlled by temperature and decreases with increasing temperatures. In this study, the results show that $\Delta_r G_m^{\Theta}$ of Eq. (1) decreases gradually as the temperature increases from 50 to 800 °C, suggesting elevated temperature facilitates the hydrolysis reaction of Eq. (1) towards the right and weakens the stability and transport of the Ru-Cl complex. $\Delta_r G_m^{\Theta}$ of the reaction of Eq. (1) is still positive when the temperature goes up to 800 °C, indicating the reaction is endothermic and cannot happen autonomously at high temperatures. Therefore, the hydrolysis of Ru-Cl complex is an endothermic reaction in which a low-temperature environment will be good for the stability of the Ru-Cl complex.

3.4. Geochemical modeling

Considering the simplicity of the experimental solutions of K_2RuCl_6 and the complexity of natural fluids in which anions and anion groups of great variety are involved (Brugger et al., 2016; Ding et al., 2018), we carried out a geochemical modeling for the Ru mobility in natural Cl-rich hydrothermal fluids to quantitatively discuss the influence of temperature, chloride concentration, and pH. Two assumptions were proposed for the simulation: (1) only three equivalent compounds containing the chlorine, i.e., HCl, Cl^-, and the $RuCl_6^{2-}$ complex, were involved in the calculations, while the other complexes or compounds containing the chlorine were considered to be equivalent to the chloride ion Cl^- in hydrothermal fluids; (2) Sufficient ruthenium is available.

Based on the two assumptions above, we established a formula for the total chlorine content in a given system:

$$c(Cl_t) = c(HCl) + c(Cl^-) + c(Cl_{Ru}) \tag{9}$$

where $c(Cl_t)$, $c(HCl)$, $c(Cl^-)$, and $c(Cl_{Ru})$ represent the equivalent concentrations of the total chlorine, hydrochloric acid, chloride ion, and the Ru-Cl complex, respectively. The activity co-efficient (γ) and the dissociation constant of HCl (K_{HCl}) (Mei et al., 2018) were introduced into Eq. (9), and it was rewritten as

$$[\mathrm{Cl}^-] = \frac{\mathrm{c}(\mathrm{Cl_t}\ ) - \frac{6[\mathrm{RuCl}_6^{2-}]}{\gamma_{\mathrm{RuCl}_6^{2-}}}}{\frac{[\mathrm{H}^+]}{\mathrm{K_{HCl}}} + \frac{1}{\gamma_{\mathrm{Cl}^-}}}. \tag{10}$$

And Eq. (10) can be introduced into Eq. (4), and it was rewritten as

$$K = \frac{[HCl]^4 \times [Cl^-]^2}{\left[RuCl_6^{2-}\right]} = \frac{[H^+]^4 \times [Cl^-]^6}{{K_{HCl}}^4\left[RuCl_6^{2-}\right]} = \frac{\left\{\frac{c(Cl_t) - \frac{6\left[RuCl_6^{2-}\right]}{\gamma RuCl_6^{2-}}}{\frac{[H^+]}{K_{HCl}} + \frac{1}{\gamma_{Cl^-}}}\right\}^6 [H^+]^4}{K_{HCl}^4\left[RuCl_6^{2-}\right]} \tag{11}$$

where K, γ_{Cl^-}, and $\gamma_{\mathrm{RuCl}_6^{2}}$- are functions of temperature at a given pressure and can be attained in this study, while $[H^+]$ is equivalent to the fluid's pH. In Eq. (11), the concentrations of the Ru-Cl complex and chloride ion Cl^- in the fluids, as well as the pH, are subject to two equilibrium reactions and their equilibrium constants ($K_{\mathrm{RuCl}_6^{2-}}$ and K_{HCl}) therein. Therefore, we can use the VBA programming in Excel to solve the Eq. (11) by a batch single variable.

Given a constant $c(Cl_t)$ and pH, the concentration of Ru-Cl complex, equivalent to the mobility of Ru or its complex, varies with temperature (Figs. 6 and 7). At the acidic conditions, the mobility of Ru fluctuates significantly at temperatures from 200 to 600 °C, reaching the maximum and the minimum at ~ 500 °C and ~ 300 °C, respectively, in a low-chlorine (≤0.1 wt%) fluids. In the high-chlorine (≥0.5 wt%) fluids, the mobility of Ru is primarily controlled by the chlorine concentration rather than temperature (Fig. 6a). In the neutral to alkaline

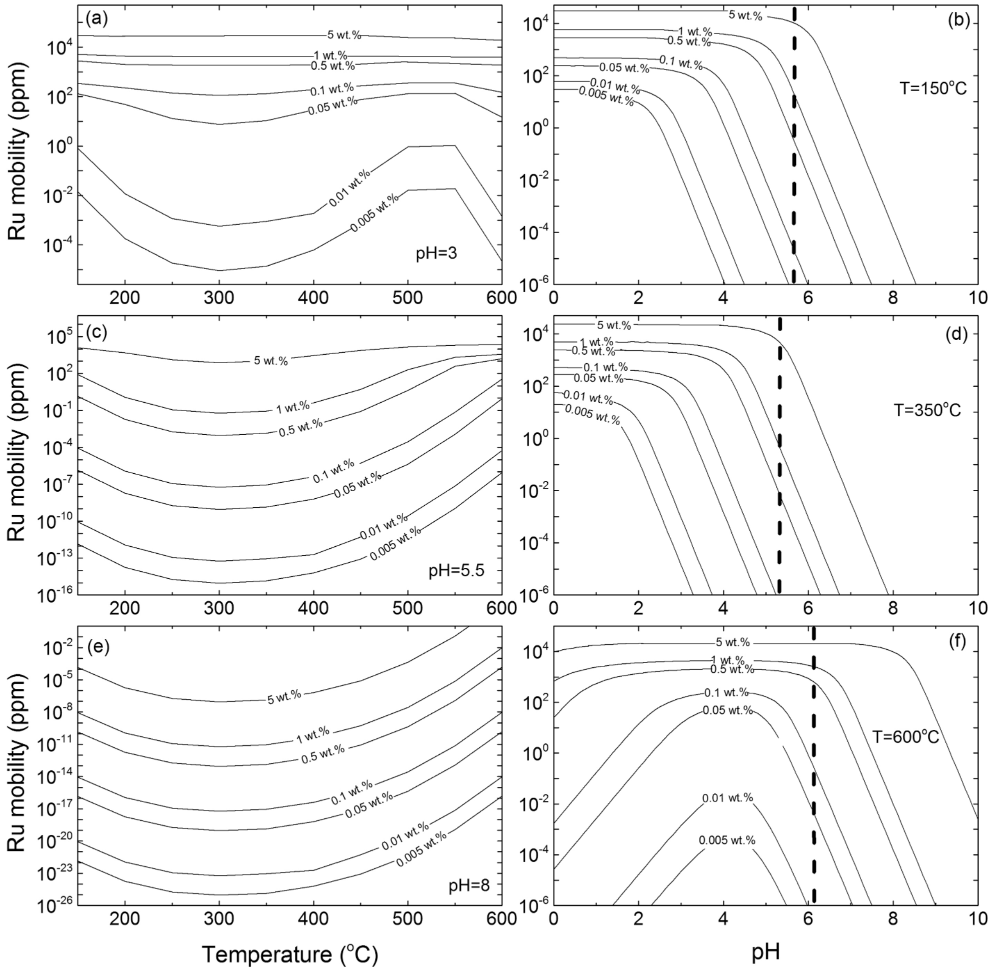

Fig. 6. Temperature-Ru mobility and pH-Ru mobility diagrams showing how the Ru concentration varies with increasing temperature (200 to 600 °C), pH (0 to 10), and Cl concentration in the hydrothermal fluids (0.005 wt% to 5 wt%). The dotted line represents the neutral fluid at elevated temperatures.

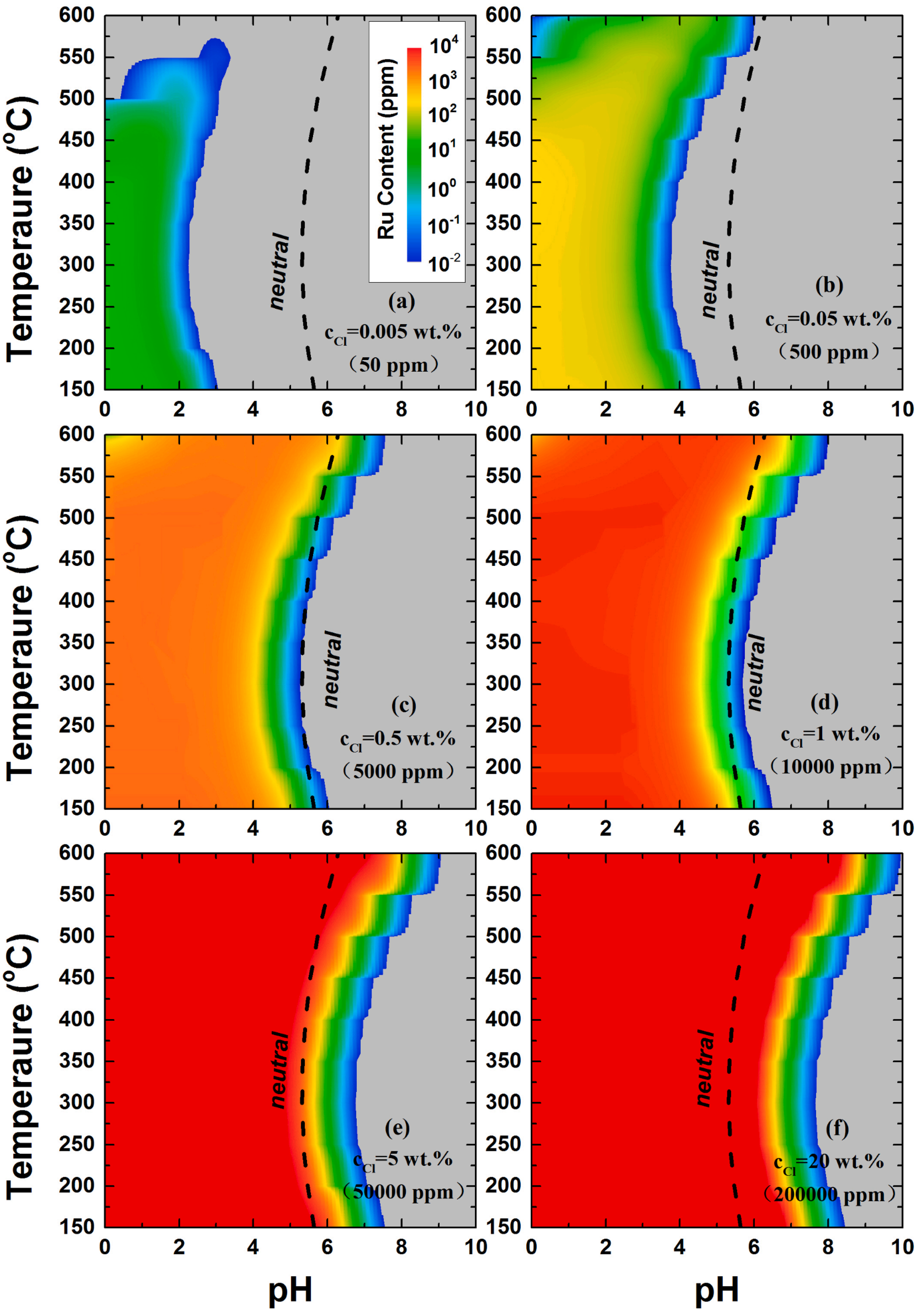

Fig. 7. pH-Temperature diagrams illustrating the variations of Ru concentration with increasing temperature, pH, and Cl concentration in the hydrothermal fluids.

hydrothermal fluids, the mobility of Ru first decreases and then increases with temperature from 200 to 600 °C, reaching the minimum at ~300 °C (Fig. 6c, 6e). In addition to temperature, pH has significant effects on the mobility of Ru in the fluids. As shown in Fig. 6b and 6d, at low to moderate temperatures (≤350 °C), with the pH increasing from 0 to 10, the mobility of Ru remains stable firstly and then decreases monotonically, indicating acidic fluids promote the transport of Ru. By contrast, at high temperatures (≥600 °C), the mobility of Ru increases firstly and then decreases with increasing pH, peaking at pH of ~ 4, suggesting that high temperature shifts the optimal pH for the mobility of Ru from acidic towards weakly acidic (Fig. 6f). Nevertheless, it is noteworthy that no matter how temperature and pH change, the mobility of Ru is dominated mainly by the total chlorine concentration and increases by orders of magnitude with increasing chlorine in fluids (Fig. 6).

Overall, the Ru-Cl complex could be transported in large quantities in acidic ($pH \leq 4$) hydrothermal fluids of low to moderate temperatures ($\leq$500 °C) and high chlorine concentrations ($\geq$0.5 wt%) (Fig. 7). In low-chlorine ($\leq$0.05 wt%) hydrothermal fluids, the Ru-Cl complex remains stable at low to moderate temperatures ($\leq$500 °C) and acidity ($pH \leq 4$), with maximum mobility of about hundreds of ppm (Fig. 7a-b). With the chlorine concentration increasing ($\geq$0.5 wt%), the Ru-Cl complex can be stable on a much more extensive range of temperature ($\leq$600 °C or higher) and pH ($\leq$6). Correspondingly, the mobility of the Ru-Cl complex is higher, up to thousands of ppm in the hydrothermal fluids (Fig. 7c-f). Similar to the Pt behavior in Cl-rich hydrothermal fluids (Hsu et al., 1991), the Ru concentration decreases gradually with increasing temperatures, but increases by orders of magnitude when sufficient chloride and low pH are available in the fluids, indicating that the high chlorine concentration and low pH can greatly enhance the Ru mobility in the hydrothermal fluids (Fig. 7). More importantly, when the total chlorine concentration in fluids is high enough ($\geq$5 wt%), the stability and mobility of Ru-Cl complex could be extended from the low pH (acidic) to high pH (weakly alkaline) range and is almost irrelative to the temperature (Fig. 7e, f). This further confirms the key role of total chlorine concentration in fluids on the Ru hydrothermal mobility.

4. Geological implications

As numerous field observations and experiments have shown, PGE can be transported in the form of PGE-Cl complexes in magmatic-hydrothermal fluids, especially in the Cl-rich fluids, and eventually be precipitated wherever physicochemical conditions change (Hekinian et al., 1980; Wood et al., 1989; Mckibben et al., 1990; Xiong and Wood, 2000; Kazachenko et al., 2006; Holwell et al., 2017; Mcfall et al., 2018). This study further demonstrates that Ru could be mobile in the Cl-bearing (0.05–0.5 wt%), low to moderate temperature ($\leq$550 °C), and acidic ($pH \leq 4$) fluids, and be highly mobile in the Cl-rich (0.5–20 wt%), acidic - weakly alkaline fluids in which temperature effect is ignorable (Fig. 7). More importantly, although the Ru-Cl complex should strongly hydrolyze and be extremely unstable in fluids at elevated temperatures and pressures, its hydrolysis behavior will be restrained effectively when the fluids have low pH and, in particular high chlorine concentration. Such regulation on the Ru-Cl complex's hydrolysis and inhibition could be the primary mechanism behind the PGE mobilization, transport, and deposition in the hydrothermal fluids that might happen in submarine hydrothermal vent systems.

Usually, submarine hydrothermal fluids have high chloride concentration (up to 4.2 wt%), low pH (2.1–3.5), and moderate temperature (up to 375 °C) in the mid-ocean ridge regions (Delaney et al., 1992; Zeng et al., 2016). Under this kind of fluid circumstance, ruthenium in deep magma derived from the mantle and surrounding oceanic crust could be massively extracted into the fluids (Yan et al., 2003; Li and Yan, 2013) to form the high coordination Ru-Cl complexes (Chen. 1994). As demonstrated by this study, due to the Ru-Cl complexes' stability, ruthenium would be enriched in the magmatic-hydrothermal fluids to over 10,000 ppm (Fig. 6a, 7e) if the source is capable of supplying enough Ru. With the Ru-rich hydrothermal fluids rising driven by the magma heat, it could be mixed with penetrating seawater that has low chloride concentrations (~1.9 wt%) and high pH (8–10) (Robigou et al., 1993; Butterfield et al., 1994; Lilley et al., 1995; Hansen, 2002; Hinga, 2002; Middelboe and Hansen, 2007). This process that happens within the hydrothermal chimneys will cause the temperature and chlorine concentration of the fluids decline, as well as the pH rise, such that the Ru-Cl complex's stability is gradually lowered, and its mobility is most likely to be reduced by one order of magnitude (Fig. 6a). This can plausibly explain the PGE precipitation and enrichment observed in hydrothermal chimneys of the mid-ocean ridges (Harrar and Stephens, 1984; Mckibben et al., 1990; Huang et al., 2011).

However, before the pH is elevated to 6 (Fig. 6d), the magmatic-hydrothermal fluids in the hydrothermal vent systems still have great capability to transport several ppm - several thousand ppm Ru in theory, which makes it possible to transport the PGE to the regions nearby the vents or even the farther places. Due to the buoyancy, the emitted hydrothermal vent fluids continue rising to form hydrothermal plume by the turbulent mixing with ambient seawater (e.g., Baker, 1994; Speer and Rona, 1989). It has been observed that the hydrothermal plume can ascend and/or spread laterally over distances of a few kilometers to hundreds of kilometers (Lupton and Craig, 1981; Baker, 1994; Resing et al., 2015). During this process, the hydrothermal plume continues to be diluted until its component becomes homogeneous to the ambient seawater (Speer and Rona, 1989). Correspondingly, the Ru-Cl complex's stability and mobility also decline rapidly when the plume pH is elevated to over 6 (Figs. 6, 7). Finally, the Ru-Cl complex accomplishes its task of transporting Ru from the deep magma chamber to the seafloor. Because of the enhanced unstability of the Ru-Cl complex during the hydrothermal plume spreading, the dissolved Ru is rapidly hydrolyzed in a certain region, most likely leading to Ru enrichment in the submarine muds, encrustations, nodules, and sulfides (He et al., 2006; Ren et al., 2016). In this respect, the pH elevating rate rather than the spreading capability of the hydrothermal plume decides the PGE transport even if the ambient seawater is enriched in the chlorine (Fig. 7).

It is noteworthy that when the hydrothermal plume's pH changes to be neutral or alkaline, it does not mean that Ru is entirely inactive. Previous experimental studies on the Pt and Pd speciation in Cl-bearing solutions have demonstrated that the dominant species in the fluids whose Cl^- activity is analogue to the seawater will transform from the high coordination PGE-Cl complexes to the hydroxide ones when the pH is more than 6 (Wood et al., 1992). This implies that a portion of dissolved Ru will occur in the plume or ambient seawater in the form of the hydroxide complexes, i.e., $Ru(OH)_4^0$, $Ru(OH)_5^-$, etc. (Yan et al., 2020a). Given that the Ru-OH complexes are mostly low solubility and readily to dehydrate (Sassani and Shock, 1998), their capability of transporting Ru is much lower than those of the Ru-Cl complexes.

It is the other remarkable fact that the Ru concentration in most natural minerals, fluids, and rocks is less than several ppm, even though our geochemical modeling inferred that Ru dissolved and transported by the Cl-rich, acidic, and low-moderate temperature fluids could be up to thousands of ppm. This could be mostly attributed to the Ru deficiency in the sources. The abundance of Ru in the primitive mantle and continental crust is 5 and 0.2–1 ppt (Li, 1976; Mcdonough and Sun, 1995; Gao et al., 1998), respectively. The magmas generated from the mantle (e.g., (ultra)-mafic rocks) usually contain elevated ruthenium (0.1–2.36 ppb) (Li, 1976; Song et al., 2009; Yan et al., 2020a). Ruthenium is extracted from the magmas and enters the magmatic-hydrothermal fluids, during which it could be enriched in the hydrothermal minerals by several orders of magnitude as an isomorphism in the place of iron and cobalt or intermetallic compound (Liu et al., 1984, 2007; Yan et al., 2020a), such as the Cu-rich stockwork ores (Ru up to 21 ppb) of the Aguas Teñidas Este (Pašava et al., 2007), the ores (Ru 0.2–6 ppb) of massive sulfide deposits (Vikentyev et al., 2004), the pentlandite-pyrrhotite-pyrite-chalcopyrite (Ru 0.47–12.14 ppm) from the Grasvally-Norite-Pyroxenite-Anorthosite (GNPA) Member, northern Bushveld Complex (Holwell et al., 2017). OIB and MORB also contain low ruthenium (~2 ppt) and can provide very limited Ru for hydrothermal fluids (Song et al., 2009). However, hydrothermal vent fluids can concentrate Ru to 44 ppt by at least one order of magnitude (Huang et al., 2011) while submarine encrustations and minerals can concentrate Ru to tens or hundreds of ppb by four or five orders of magnitude (He et al., 2006; Asavin et al., 2008; Ren et al., 2016). Hence, even if Ru could be concentrated by several orders of magnitude through the Cl-rich and acidic hydrothermal activities, the Ru transport and enrichment in most geological environments is greatly limited by the Ru deficiency in the sources, resulting in the scarcity of hydrothermal Ru deposits in the crust.

5. Conclusion

In order to better understand thermodynamic properties of the PGE chloride complexes and the PGE circulation, we conducted a series of hydrolysis experiments between $RuCl_6^{2-}$ and water at 200 to 600 °C, 100 MPa, as well as modeling the mobility of the complex in the natural Cl-bearing hydrothermal fluids by establishing a preliminary quantitative model. Kinetic equilibrium experiments showed that the cumulative hydrolysis reaction got equilibrium within 24 hours, suggesting the hydrolysis of the Ru-Cl complex is much faster than mineral dissolution. Temperature-series hydrolysis experiments displayed that temperature had a positive effect on the $RuCl_6^{2-}$ hydrolysis, such that the hydrolysis intensity and cumulative hydrolysis constants increased with increasing temperatures. A function of the cumulative hydrolysis constants and temperature (K, Kelvin) was obtained using the Debye-Hückel and Van't Hoff equations:

$$lnK = (42.95 \pm 4.13) - -(56205 \pm 2594)/T,$$

where $\Delta_r H_m^{\Theta}$ and $\Delta_r S_m^{\Theta}$ were calculated to be (467.3 ± 21.56) $kJ{\cdot}mol^{-1}$ and (357.1 ± 34.37) $J{\cdot}mol^{-1}{\cdot}K^{-1}$, respectively. Correspondingly, $\Delta_r G_m^{\Theta}$ of the hydrolysis reaction decreases from (351.92 ± 9.47) $kJ{\cdot}mol^{-1}$ at 50 °C to (84.10 ± 18.67) $kJ{\cdot}mol^{-1}$ at 800 °C.

Based on the cumulative hydrolysis constants obtained in this study, the quantitative geochemical modeling demonstrated that Ru could be mobile in the Cl-bearing (0.05–0.5 wt%), low to moderate temperature ($\leq$550 °C), and acidic (pH $\leq$ 4) fluids, and be highly mobile in the Cl-rich (0.5–20 wt%), acidic - weakly alkaline fluids with an ignorable temperature effect. Elevating pH will promote the hydrolysis of the Ru-Cl complex and lower the Ru mobility in fluids. In contrast, higher chlorine concentration in fluids can inhibit the hydrolysis and enhance Ru transport by several orders of magnitude. Therefore, the hydrolysis and inhibition for the PGE-Cl complex could be the primary mechanism controlling the PGE mobilization, transport, and deposition in the Cl-bearing hydrothermal fluids.

The Cl-rich and acidic hydrothermal fluids derived from the deep magma are capable of extracting and transporting a large amount of Ru continuously with regard to the hydrothermal vent systems in mid-ocean ridge regions. Ascending hydrothermal fluids and subsequently emitted plumes are gradually diluted by ambient seawater, leading to the chlorine concentration decline and the pH rise. This critical process will primarily reduce the Ru mobility and induce the Ru deposition within the hydrothermal chimneys and other regions covered by the hydrothermal plumes. When the fluid's pH is elevated to be weakly alkaline, the Ru-Cl complex accomplishes its task of transporting Ru from the deep to the seafloor.

Declaration of Competing Interest

The authors declare that they have no known competing financial interests or personal relationships that could have appeared to influence the work reported in this paper.

Acknowledgments

We thank the reviewers and Prof. Franco Pirajno for their constructive comments and suggestions. This study was supported by the Strategic Priority Research Program of the Chinese Academy of Sciences (XDB42000000), the National Key R&D Program of China (2016YFC0600408), and the National Natural Science Foundation of China (41730423, 41773054). This is contribution No. IS-2978 from GIGCAS.

Appendix A. Supplementary data

Supplementary data to this article can be found online at https://doi.org/10.1016/j.oregeorev.2021.104043.

References

Asavin, A.M., Anikeeva, L.I., Kazakova, V.A., Andreev, S.I., Sapozhnikov, D.A., Roshchina, I.A., et al., 2008. Trace element and PGE distribution in layered ferromanganese crusts. Geochem. Int. 46, 1179–1205. https://doi.org/10.1134/s001670290812001x.

Auge, T., Petrunov, R., Bailly, L., 2005. On the origin of the PGE mineralization in the Elatsite porphyry Cu-Au deposit, Bulgaria; comparison with the Baula-Nuasahi Complex, India, and other alkaline PGE-rich porphyries. Can. Mineralogist 43, 1355–1372. https://doi.org/10.2113/gscanmin.43.4.1355.

Baes, J.C.F., Mesmer, R.E., 1981. The thermodynamics of cation hydrolysis. Am. J. Sci. 281, 935–962.

Baker, E.T., 1994. A 6-year time series of hydrothermal plumes over the Cleft segment of the Juan de Fuca Ridge. J. Geophys. Res. Solid Earth 99, 4889.

Barnes, S.J., Liu, W.H., 2012. Pt and Pd mobility in hydrothermal fluids: Evidence from komatiites and from thermodynamic modelling. Ore Geol. Rev. 44, 49–58.

Barnes, S.J., Makovicky, E., Makovicky, M., Rosehansen, J., Karupmoller, S., 1997. Partition coefficients for Ni, Cu, Pd, Pt, Rh, and Ir between monosulfide solid solution and sulfide liquid and the formation of compositionally zoned Ni – Cu sulfide bodies by fractional crystallization of sulfide liquid. Revue Canadienne Des Sciences De La Terre 34, 366–374.

Brugger, J., Liu, W., Etschmann, B., Mei, Y., Sherman, D.M., Testemale, D., 2016. A review of the coordination chemistry of hydrothermal systems, or do coordination changes make ore deposits? Chem. Geol. 447, 219–253. https://doi.org/10.1016/j.chemgeo.2016.10.021.

Butterfield, D.A., McDuff, R.E., Mottl, M.J., Lilley, M.D., Lupton, J.E., Massoth, G.J., 1994. Gradients in the composition of hydrothermal fluids from the Endeavour segment vent field: Phase separation and brine loss. J. Geophys. Res. Solid Earth 99, 9561–9583. https://doi.org/10.1029/93JB03132.

Chen, J., 1994. Classification and solubility regularity of insoluble coorination compounds of platinum group metals. Precious Metals 15, 15–24 (in Chinese with English abstract).

Coveney, R.M., Nansheng, C., 1991. Ni-Mo-PGE-Au-rich ores in Chinese black shales and speculations on possible analogues in the United States. Mineral Deposita 26, 83–88. https://doi.org/10.1007/BF00195253.

Crocket, J.H., 1979. Platinum-group elements in mafic and ultramafic rocks: A survey. Can. Mineral. 17, 391–402.

Delaney, J.R., Robigou, V., Mcduff, R.E., Tivey, M.K., 1992. Geology of a vigorous hydrothermal system on the Endeavour Segment, Juan de Fuca Ridge. J. Geophys. Res. Solid Earth 97, 19663–19682. https://doi.org/10.1029/92JB00174.

Ding, X., Harlov, D.E., Chen, B., Sun, W.D., 2018. Fluids, metals, and mineral/ore deposits. Geofluids 2018, 1452409. https://doi.org/10.1155/2018/1452409.

Douglas, B.E., Ho, S.M., 2006. Crystal structures involving P and T layers. In: Structure and Chemistry of Crystalline Solids. Springer, New York, pp. 117–146. https://doi.org/10.1007/0-387-36687-3_6.

Gammons, C.H., 1995. Experimental investigations of the hydrothermal geochemistry of platinum and palladium: IV. The stoichiometry of Pt (IV) and Pd (II) chloride complexes at 100 to 300°C. Geochim. Cosmochim. Acta 59, 1655–1667. https://doi.org/10.1016/0016-7037(95)00074-A.

Gammons, C.H., Bloom, M.S., 1990. Experimental investigations on the stability and stoichiometry of Pd(II), Pt(II) and Pt(IV) chloride complexes to 300°C. Geol. Soc. Am. 22, A158.

Gammons, C.H., Bloom, M.S., 1993. Experimental investigation of the hydrothermal geochemistry of platinum and palladium: II. The solubility of PtS and PdS in aqueous sulfide solutions to 300°C. Geochim. Cosmochim. Acta 57, 2451–2467.

Gammons, C.H., Bloom, M.S., Yu, Y., 1992. Experimental investigation of the hydrothermal geochemistry of platinum and palladium: I. Solubility of platinum and palladium sulfide minerals in NaCl/H2SO4 solutions at 300°C. Geochim. Cosmochim. Acta 56, 3881–3894. https://doi.org/10.1016/0016-7037(92)90003-2.

Gao, S., Luo, T.C., Zhang, B.R., Zhang, H.F., Han, Y.W., Zhao, Z.D., et al., 1998. Chemical composition of the continental crust as revealed by studies in East China. Geochim. Cosmochim. Acta 62, 1959–1975.

Garrels, R.M., Christ, C.L., 1965. In: Solutions, Minerals, and Equilibria. Harper & Row, New York, pp. 1–450.

Halbach, P., Kriete, C., Prause, B., Puteanus, D., 1989. Mechanisms to explain the platinum concentration in ferromanganese seamount crusts. Chem. Geol. 76, 95–106.

Hanley, J.J., Pettke, T., Mungall, J.E., Spooner, E.T.C., 2005. The solubility of platinum and gold in NaCl brines at 1.5 kbar, 600 to 800°C: A laser ablation ICP-MS pilot study of synthetic fluid inclusions. Geochim. Cosmochim. Acta 69, 2593–2611. https://doi.org/10.1016/j.gca.2004.11.005.

Hansen, P.J., 2002. Effect of high pH on the growth and survival of marine phytoplankton: Implications for species succession. Aquatmicrobecol 28, 279–288. https://doi.org/10.3354/ame028279.

Harrar, J.E., Stephens, F.B., 1984. Recovery of Platinum from Concentrated Sodium Chloride Brine by Electrodeposition on Vitreous Carbon. Lawrence Livermore National Lab, CA, USA.

He, G.W., Sun, X.M., Yang, S.X., Xue, T., Song, C.B., Shi, G.Y., et al., 2006. Platinum group elements (PGE) geochemistry of polymetallic nodules in CC zone, east Pacific Ocean. Mineral Deposits 25, 164–174 (in chinese with English abstract).

He, J.J., Ding, X., Wang, Y.R., Sun, W.D., 2015a. The effect of temperature and concentration on hydrolysis of fluorine-rich titanium complexes in hydrothermal fluids: Constraints on titanium mobility in deep geological processes. Acta Petrol. Sin. 31, 802–810 (in Chinese with English abstract).

He, J.J., Ding, X., Wang, Y.R., Sun, W.D., 2015b. The effects of precipitation-aging-re-dissolution and pressure on hydrolysis of fluorine-rich titanium complexes in hydrothermal fluids and its geological implications. Acta Petrol. Sin. 31, 1870–1878 (in Chinese with English abstract).

Hekinian, R., Fevrier, M., Bischoff, J.L., Picot, P., Shanks, W.C., 1980. Sulfide deposits from the East Pacific Rise near 21°N. Science 207, 1433–1444.

Helgeson, H.C., Kirkham, D.H., 1974. Theoretical prediction of the thermodynamic behavior of aqueous electrolytes at high pressures and temperatures; II, Debye-Huckel parameters for activity coefficients and relative partial molal properties. Am. J. Sci. 274, 1089–1198.

Helgeson, H.C., Kirkham, D.H., Flowers, G.C., 1981. Theoretical prediction of the thermodynamic behavior of aqueous-electrolytes at high-pressures and temperatures: IV. Calculation of activity-coefficients, osmotic coefficients, and apparent molal and standard and relative partial molal properties to 600°C and 5 KB. Am. J. Sci. 281, 1249–1516.

Hinga, K.R., 2002. Effects of pH on coastal marine phytoplankton. Marine Ecol. Prog. 238, 281–300. https://doi.org/10.3354/meps238281.

Hoatson, D.M., Keays, R.R., 1989. Formation of platiniferous sulfide horizons by crystal fractionation and magma mixing in the Munni Munni Layered intrusion, West Pilbara Block, Western Australia. Econ. Geol. 84, 1775–1804.

Holovko, M., Druchok, M., Bryk, T., 2005. Primitive model for cation hydrolysis: A molecular-dynamics study. J. Chem. Phys. 123, 154505.

Holovko, M., Druchok, M., Bryk, T., 2009. Cation hydrolysis phenomenon in aqueous solution: Towards understanding it by computer simulations. Springer 221–253.

Holwell, D.A., Adeyemi, Z., Ward, L.A., Smith, D.J., Graham, S.D., Mcdonald, I., et al., 2017. Low temperature alteration of magmatic Ni-Cu-PGE sulfides as a source for hydrothermal Ni and PGE ores: a quantitative approach using automated mineralogy. Ore Geol. Rev. 91, 718–740.

Hsu, L.C., Lechler, P.J., Nelson, J.H., 1991. Hydrothermal solubility of palladium in chloride solutions from 300° to 700°C: Preliminary experimental results. Econ. Geol. 86, 422–427.

Huang, W., Li J., Tao C.H., Sun Z.L., He Y.J., Cui N.Y. 2011. PGE characteristics of sulfide chimney bodies in hydrothermal regions, Southwest Indian ridge 49 ° 39 `E. Acta Mineralogica Sinica Z, 691 (in chinese).

Hurtig, N.C., Williams-Jones, A.E., 2014. An experimental study of the solubility of MoO3 in aqueous vapour and low to intermediate density supercritical fluids. Geochim. Cosmochim. Acta 136, 169–193. https://doi.org/10.1016/j.gca.2014.03.043.

Kazachenko, V.T., Miroshnichenko, N.V., Perevoznikova, E.V., Karabtsov, A.A., 2006. Sikhote Alin as a possible province of hydrothermal sedimentary gold, silver, PGE, tin, zinc, lead, and tungsten deposits. Dokl. Earth Sci. 410, 1007–1013.

Keays, R.R., 1995. The role of komatiitic and picritic magmatism and S-saturation in the formation of ore deposits. Lithos 34, 1–18.

Keays, R.R., Davison, R.M., 1976. Palladium, iridium, and gold in the ores and host rocks of nickel sulfide deposits in Western Australia. Econ. Geol. 71, 1214–1228.

Kielland, J., 1937. Individual activity coefficients of ions in aqueous solutions. J. Am. Chem. Soc. 59, 1675–1678.

Lefort, D., Hanley, J.J., Marcel, G., 2011. Subepithermal Au-Pd mineralization associated with an alkalic porphyry Cu-Au deposit, Mount Milligan, Quesnel Terrane, British Columbia, Canada. Econ. Geol. 106, 781–808. https://doi.org/10.2113/econgeo.106.5.781.

Levitin, G., Schmuckler, G., 2003. Solvent extraction of rhodium chloride from aqueous solutions and its separation from palladium and platinum. React. Funct. Polym. 54, 149–154.

Li, R.P., Yan, J.D., 2013. Hydrothermal fluids and ore genesis of PGE. Contrib. Geol. Mineral Resour. Res. 28, 335–343 (in Chinese with English abstract).

Li, T., 1976. Chemical element abundances in the earth and it's major shells. Geochimica 167–174 (in Chinese with English abstract).

Lilley, M.D., Feely, R.A., Trefry, J.H., 1995. Chemical and biochemical transformations in hydrothermal plumes. Geophys. Monogr. 91, 369–391. https://doi.org/10.1029/GM091p0369.

Liu, S.Q., Shi, Y.Z., Zhu, R.H., 2007. Development of species analysis of platinum group element. Chin. J. Spectroscopy Lab. 24, 43–49 (in Chinese with English abstract).

Liu, Y.J., Cao, L.M., Li, Z.L., Wang, H.N., Chu Zhang J.R., T.Q., 1984. In: Elemental Geochemistry. Science Press, Beijing, pp. 1–548 (in Chinese).

Lupton, J.E., Craig, H., 1981. A major helium-3 source at 15 S on the East Pacific Rise. Science 214, 13–18. https://doi.org/10.1126/science.214.4516.13.

Mar, S.Y., Chen, C.S., Huang, Y.S., Tiong, K.K., 1995. Characterization of RuO_2 thin films by Raman spectroscopy. Appl. Surf. Sci. 90, 497–504.

Mcdonough, W.F., Sun, S.S., 1995. The composition of the Earth. Chem. Geol. 120, 223–253.

Mcfall, K.A., Naden, J., Roberts, S., Baker, T., Spratt, J., Mcdonald, I., 2018. Platinum-group minerals in the Skouries Cu-Au (Pd, Pt, Te) porphyry deposit. Ore Geol. Rev. 99, 344–364.

Mckibben, M.A., Williams, A.E., Hall, G.E.M., 1990. Solubility and transport of platinum-group elements and Au in saline hydrothermal fluids - Constraints from geothermal brine data. Econ. Geol. Bull. Soc. 85, 1926–1934. https://doi.org/10.2113/gsecongeo.85.8.1926.

Mei, Y., Liu, W., Brugger, J., Sherman, D.M., Gale, J.D., 2018. The dissociation mechanism and thermodynamic properties of HCl (aq) in hydrothermal fluids (to 700 °C, 60 kbar) by ab initio molecular dynamics simulations. Geochim. Cosmochim. Acta 226, 84–106.

Middelboe, A.L., Hansen, P.J., 2007. High pH in shallow-water macroalgal habitats. Mar. Ecol. Prog. 338, 107–117. https://doi.org/10.3354/meps338107.

Migdisov, A.A., Williams-Jones, A.E., 2007. An experimental study of the solubility and speciation of neodymium (III) fluoride in F-bearing aqueous solutions. Geochim. Cosmochim. Acta 71, 3056–3069. https://doi.org/10.1016/j.gca.2007.04.004.

Migdisov, A.A., Williams-Jones, A.E., van Hinsberg, V., Salvi, S., 2011. An experimental study of the solubility of baddeleyite (ZrO2) in fluoride-bearing solutions at elevated temperature. Geochim. Cosmochim. Acta 75, 7426–7434. https://doi.org/10.1016/j.gca.2011.09.043.

Mo, J.X., 2004. Impact on chemistry reaction speed, balance and conversion ratio of temperature. Higher Educ. Forum 5, 161–164 (In chinese with English abstract).

Mountain, B.W., Wood, S.A., 1988a. Chemical controls on the solubility, transport and deposition of platinum and palladium in hydrothermal solutions: A thermodynamic approach. Econ. Geol. 83, 492–510.

Mountain, B.W., Wood, S.A., 1988b. In: Solubility and Transport of Platinum-Group Elements in Hydrothermal Solutions: Thermodynamic and Physical Chemical Constraints. Springer, Netherlands, pp. 57–82.

Naldrett, A.J. 2004. Platinum group element (PGE) deposits. In: Naldrett, A.J. (ed.). Magmatic Sulfide Deposits: Geology, Geochemistry and Exploration. Berlin, Heidelberg: Springer. pp. 481–612. https://dx.doi.org/10.1007/978-3-662-08444-1_9.

Naldrett, A.J., Ebel, D.S., Asif, M., Morrison, G., Moore, C.M., 1997. Fractional crystallisation of sulfide melts as illustrated at Noril'sk and Sudbury. Eur. J. Mineral. 9, 365–377.

Orlova, G.P., Ryabchikov, I.D., Distler, V.V., Gladyshev, G.D., 1987. Platinum migration in fluids during the formation of magmatic sulfides. Int. Geol. Rev. 29, 360–362.

Pan, P., Wood, S.A., 1994. Solubility of Pt and Pd sulfides and Au metal in aqueous bisulfide solutions. Miner. Deposita 29, 373–390.

Pasava, J., Frimmel, H., Taiyi, L., Koubova, M., Martinek, K., 2010. Extreme PGE concentrations in Lower Cambrian acid tuff layer from the Kunyang phosphate deposit, Yunnan Province, south China; possible PGE source for Lower Cambrian Mo-Ni-polyelement ore beds. Econ. Geol. 105, 1047–1056. https://doi.org/10.2113/econgeo.105.6.1047.

Pašava, J., Vymazalová, A., Petersen, S., Herzig, P., 2004. PGE distribution in massive sulfides from the P ACMANUS hydrothermal field, eastern Manus basin, Papua New Guinea: implications for PGE enrichment in some ancient volcanogenic massive sulfide deposits. Miner. Deposita 39, 784–792.

Pašava, J., Vymazalová, A., Tornos, F., 2007. PGE distribution in massive sulfide deposits of the Iberian Pyrite Belt. Miner. Deposita 42, 309–314.

Persson, K. 2016, Materials Data on K2RuCl6 (SG:225) by Materials Project, https://dx.doi.org/10.17188/1199529.

Ren, J.B., He, G.W., Yao, H.Q., Zhang, H.D., Yang, S.X., Deng, X.G., et al., 2016. Geochemistry and significance of REE and PGE of the cobalt-rich crusts from west Pacific Ocean Seamounts. Earth Sci. 41, 1745–1757 (in Chinese with English abstract).

Resing, J.A., Sedwick, P.N., German, C.R., Jenkins, W.J., Moffett, J.W., Sohst, B.M., et al., 2015. Basin-scale transport of hydrothermal dissolved metals across the South Pacific Ocean. Nature 523, 200–203. https://doi.org/10.1038/nature14577.

Robigou, V., Delaney, J.R., Stakes, D.S., 1993. Large massive sulfide deposits in a newly discovered active hydrothermal system, The high-rise field, endeavour segment, Juan De Fuca Ridge. Geophys. Res. Lett. 20, 1887–1890. https://doi.org/10.1029/93gl01399.

Sassani, D.C., Shock, E.L., 1998. Solubility and transport of platinum-group elements in supercritical fluids: summary and estimates of thermodynamic properties for ruthenium, rhodium, palladium, and platinum solids, aqueous ions, and complexes to 1000°C and 5 kbar. Geochim. Cosmochim. Acta 62, 2643–2671.

Song, X.Y., Hu, R.Z., Chen, L.M., 2009. Geochemical natures of copper, nickel and PGE and their significance for the study of origin and evolution of mantle-derived magmas and magmatic sulfide deposits. Earth Sci. Front. 16, 287–305 (in Chinese with English abstract).

Speer, K.G., Rona, P.A., 1989. A model of an Atlantic and Pacific hydrothermal plume. J. Geophys. Res. Oceans 94, 6213–6220.

Spieker, W.A., Liu, J., Miller, J.T., Kropf, A.J., Regalbuto, J.R., 2002. An EXAFS study of the co-ordination chemistry of hydrogen hexachloroplatinate(IV): 1 Speciation in aqueous solution. Appl. Catal. A General 232, 219–235.

Tanger, J.C., Helgeson, H.C., 1988. Calculation of the thermodynamic and transport-properties of aqueous species at high-pressures and temperatures - Revised equations of state for the standard partial molal properties of ions and electrolytes. Am. J. Sci. 288, 18–98.

Timofeev, A., Migdisov, A.A., Williams-Jones, A.E., 2015. An experimental study of the solubility and speciation of niobium in fluoride-bearing aqueous solutions at elevated temperature. Geochim. Cosmochim. Acta 158, 103–111. https://doi.org/10.1016/j.gca.2015.02.015.

Timofeev, A., Migdisov, A.A., Williams-Jones, A.E., 2017. An experimental study of the solubility and speciation of tantalum in fluoride-bearing aqueous solutions at elevated temperature. Geochim. Cosmochim. Acta 197, 294–304. https://doi.org/10.1016/j.gca.2016.10.027.

Vikentyev, I., Abramova, V., Moloshag, V., Su, S., 2014. PGE in minerals of volcanogenic massive sulfide deposits of the Urals: ore geochemistry and first LA-ICP-MS data. In: Proceedings of 12th International Platinum Symposium, pp. 326–327.

Vikentyev, I.V., Yudovskaya, M.A., Mokhov, A.V., Kerzin, A.L., Tsepin, A.I., 2004. Gold and PGE in massive sulfide ore of the Uzelginsk deposit, Southern Urals, Russia. Can. Mineralogist 42, 651–665.

Wang, Y., Chou, I.M., 1987. Characteristics of hydrolysis of the complex Na2SnF6 in hydrothermal solutions—An experimental study. Chin. J. Geochem. 6, 372–382.

Wang, Y., Gu, F., Yuan, Z., 1993. Partitioning and hydrolysis of Nb and Ta and their implications with regard to mineralization. Chin. J. Geochem. 12, 84–91.

Westland, A.D., 1963. π-bonding in inorganic compounds part 5. delocalization of d-orbitals in K_2RuCl_6 and K_2OsCl_5. Can. J. Chem. 41, 2692–2695.

Wilde, A.R., Bloom, M.S., Wall, V.J., 1989. Transport and deposition of gold, uranium and platinum-group elements in unconformity-related uranium deposits. Econ. Geol. Bull. Soc. 6, 637–650.

Wood, S.A., Mountain, B.W., Fenlon, B.J., 1989. Thermodynamic constraints on the solubility of platinum and palladium in hydrothermal solutions - Reassessment of hydroxide, bisulfide, and ammonia complexing. Econ. Geol. 84, 2020–2028. https://doi.org/10.2113/gsecongeo.84.7.2020.

Wood, S.A., Mountain, B.W., Pan, P., 1992. The aqueous geochemistry of platinum, palladium and gold: Recent experimental constraints and a re-evaluation of theoretical predictions. Can. Mineralogist 30, 955–982.

Xiong, Y., Wood, S.A., 2000. Experimental quantification of hydrothermal solubility of platinum-group elements with special reference to porphyry copper environments. Miner. Petrol. 68, 1–28.

Yan, H.B., Ding, X., Wang, C.Y., Mi, M., Sun, W.D., 2020a. The mobility of Platinum-group elements in the hydrothermal fluids. Acta Petrol. Sin. 36, 85–98. https://doi.org/10.18654/1000-0569/2020.01.00 (in Chinese with English abstract).

Yan, H.B., He, J.J., Liu, X.W., Wang, H.B., Liu, J.F., Ding, X., 2020b. Thermodynamic investigation of the hydrolysis behavior of fluorozirconate complexes at 423.15–773.15 K and 100 MPa. J. Solution Chem. https://doi.org/10.1007/s10953-020-00993-1.

Yan, T., Dan, Z., Gao, Z., 2003. Study on PGE remobilization in Jinbaoshan PGE deposit. Bull. Mineral. Petrol. Geochem. 22, 32–37.

Zeng, Z.G., Zhang, Y.X., Chen, Z.X., Ma, Y., Wang, X.Y., Zhang, D.D., 2016. Geological tectonics, magmatism and seafloor hydrothermal activity in the Back-Arc basins of the Western Pacific. Studia Marina Sinica 000, 1–36 (in Chinese with English abstract).

Zheng, S., 2009. In: The Reactions of Ruthenium (II) Polypyridyl Complexes. Nelson Mandela Metropolitan University, Port Elizabeth, pp. 1–99.